"This document is intended for publication in the open literature. It is made available on the understanding that it may not be further circulated and extracts may not be published prior to publication of the original, without the consent of the Publications Officer, JET Joint Undertaking, Abingdon, Oxon, OX14 3EA, UK".

"Enquiries about Copyright and reproduction should be addressed to the Publications Officer, JET Joint Undertaking, Abingdon, Oxon, OX14 3EA".

MHD Related Transport Analysis in JET

B. Balet, G. Huysmans, M.F.F. Nave1, P. Smeulders and J.A. Wesson

JET Joint Undertaking, Abingdon, Oxfordshire, OX14 3EA
[1]Associaçao Euratom/IST, Institute Superior Technico, Lisbon, Portugal.

INTRODUCTION:

The MHD activity observed during the JET hot ion H-modes, has been described in [1]. Three main types of MHD phenomena can be distinguished:

- Core modes such as sawteeth which cause substantial drops in the core temperatures.
- Outer Modes (OM) i.e. MHD oscillations (mainly n = 1, m = 3-5) with frequencies ~ 10kHz observed within the outer 20% of the plasma.
- Giant Edge Localised Modes (ELMs).

A selection of discharges (see Table I) has been analysed with the TRANSP code to clarify the effect of the MHD instabilities on the plasma transport. For that purpose an effective χ_{eff} is defined to quantify plasma losses:

$$\chi_{eff} = q_{loss}/(n_e \nabla T_e + n_i \nabla T_i)$$

χ_{eff} doesn't separate ion and electron loss channels and includes all loss terms (conduction, convection, CX losses etc).

A typical evolution of a hot ion H-mode pulse #34500, is shown in Fig.1. The performance appears to be limited by MHD events. A saturation of the neutron yield (= 0.5 × R_{DD}), $T_e(0)$ and W_{DIA} coincides with the onset of an OM (seen in the magnetic coil signal between 12.63s and 13s). The increase in the D_α emission is correlated in time and shape to the OM. The OM is interupted by a small ELM. The plasma performance recovers until a giant ELM at t = 13.25s, which marks a drop in R_{DD} and W_{DIA}. Finally at t = 13.45s, a sawtooth combined with a giant ELM coincides with the irreversible decline of R_{DD}.

OUTER MODES:

An increase of χ_{eff} near the edge, occurs at the time of the OM (see Fig.1). However, it is not clear how they are related quantitatively. Fig.2 shows the χ_{eff} profiles before (t = 12.55s), during (t = 12.8s) and after the OM (t = 13.2s) for #34500. During the OM, χ_{eff} ($\rho \geq 0.4$)

increases by a factor 2-3. After the OM, χ_{eff} returns to values comparable to the pre-OM values. An interesting point to note is that the increase in χ_{eff} occurs over a large part of the plasma radius, even though the OM is located beyond the q = 3 surface, with displacements of 2-3 cm. However, the onset of the OM is followed by an increase in recycling, an influx of impurities and a cool front which reaches the core in ~ 20 ms (see [1]).

The increase of χ_{eff} over a larger part of the plasma radius reflects the increased loss associated with this cool front.

ELM AND SAWTOOTH:

A typical evolution of $\chi_{eff}(\rho)$ is shown in Fig.3 for #34500. χ_{eff} increases by up to 40% in the outer region at the time of an ELM (13.3s). It doesn't recover its previous value after the ELM and in fact increases further (13.4s), reaching values ~ 70% higher than 0.2 sec earler. At the time of a sawtooth combined with an ELM (13.45s) a large increase of χ_{eff} throughout the plasma radius occurs (by a factor 1.5 for $\rho < 0.8$ to 2.5 near the edge).

BALLOONING AND KINK LIMITS:

The stability plot for external kink and ballooning for #34500 shows that the plasma edge is close to marginal stability for the external kink throughout the discharge (see Fig.4). This is compatible with the observed OM. The edge pressure gradient increases along the n = 1 kink stability boundary up to the ballooning limit which is reached around the time of the maximum in R_{DD}, coincident with an ELM. This suggests that ELMs are related to ballooning modes possibly combined with external kink. The same features are seen in #33648 and #33650, but not in the highest performance pulse #33643 whose edge remains in the stable region.

HIGH FREQUENCY MODES:

A variety of high frequency coherent modes (f > 30 kHz) is observed growing throughout the H-mode phase. Some seem to be associated with a saturation of R_{DD}. Their frequencies are consistant with β-driven Alfvén eigenmodes (BAE with f ~ 60kHz) and toroidal Alfvén eigenmodes (TAE with f ~ 110-120 kHz). (see Fig.5). The χ_{eff} profiles are not affected by these modes; this may indicate that it is mainly the fast ion population which is perturbed by the high frequency modes (causing a different beam deposition profile from the TRANSP calculated one).

NON-RECOVERY:

In some circumstances, the plasma performance doesn't recover after the MHD event. This is the case for #33648 where the temperature profile T_e doesn't increase anymore once the OM has disappeared, contrary to #34500 (see Fig.1) and despite the fact that both pulses show similar amplitudes and frequecies of the OM. The only difference is that, for #34500, the OM appears 0.63 sec after the onset of NBI, whereas it appears 1.25 sec after for #33648. The flattening of the beam deposition profile with time, due to the density build-up, is a feature of all the hot-ion H-modes (see Fig.6), and in shot #33648 prevents the plasma core from reheating after the OM.

TERMINATION:

The final loss of fusion performance is triggered in most cases by an OM and/or an ELM and in the highest performance pulses by a sawtooth and/or a giant ELM (see Fig.1). This is accompanied by a large increase of P_{rad} and D_α, and by a sudden drop in R_{DD}, W_{DIA} and temperature. During this phase, $\chi_{eff}(\rho)$ increases by a factor 2-3, denoting huge thermal losses (see Fig.3). After the terminating event, the plasma doesn't reheat (see $T_e(0)$ in Fig.5) partly due to a decreasing NBI central heating (see Fig.6) and to the fact that fast ions have been expelled out of the core region by the sawtooth.

The highest fusion performance #33643 doesn't show a change in W_{DIA} at the sawtooth as large as the comparable pulse #33650. (see Fig.7). However for #33643, W_{DIA} keeps on falling after the sawtooth, suggesting a lasting change in the transport state of the plasma. This behaviour is discussed in more detail in [2].

DISCUSSION:

The 3 classes of MHD instabilities (OM, ELM and sawtooth) have a clear effect in increasing the plasma energy losses. However this effect may be partly indirect. Sawteeth affect the fast ion distribution (and therefore the NBI heating profile). The OM and ELM, although localised in the outer part of the plasma, are accompanied by changes of the temperature profile over a wider region.

The precise loss mechanism associated with the MHD instabilities is unclear. Different interpretations have been put forward, each of them accounts for part of what is observed:

1) MHD is the direct cause of the degradation in transport.

2) MHD acts as a trigger to another state of the plasma transport, which partly remains once the MHD instabilities have disappeared.

3) MHD instabilities change the recycling conditions, causing a larger influx of neutrals and therefore increasing charge-exchange losses.

The investigation of the extent of these different processes is the aim of future studies.

CONCLUSIONS:

The TRANSP analysis of individual MHD events: Outer Modes, Giant ELM and Sawtooth + ELM, shows the radial extent and the amplitudes of the loss processes, however the precise loss mechanism is not known.

The MHD instabilities have more severe consequences in the later stage of the heating phase because of decreased central heating by NBI, due to the density build-up.

REFERENCES:

[1] F. Nave, et al., 'An overview of MHD activity at the termination of JET hot ion H-modes', to be published in Nuclear Fusion.

[2] J. Wesson and B. Balet, 'Abrupt changes in confinement in the JET tokamak', submitted to Phys. Rev. Letters.

Table I:

Pul no	B (T)	I (MA)	P (MW)	β_N	H_{89P}	$\langle n_e \rangle$ ($\times 10^{19}$ m-3)	q95	κ	δ	W (MJ)	R_{DD} ($\times 10^{16}$ s^{-1})
33643	3.4	3.8	18.8	1.6	2.9	3.9	3.2	1.9	0.31	12.0	8.9
33648	3.4	3.0	16.5	1.6	2.6	3.6	3.9	1.9	0.32	8.9	5.3
33650	3.4	3.5	18.6	1.8	2.7	4.8	3.3	1.9	0.29	11.7	6.5
34500	2.7	3.1	16.0	1.9	2.5	4.0	3.3	1.9	0.32	9.0	4.0

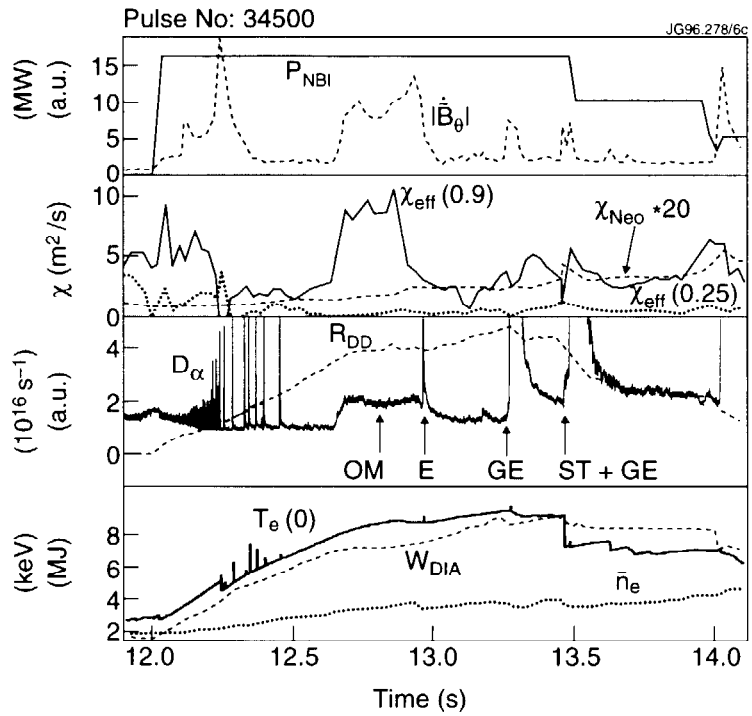

Fig. 1: Time evolution of pulse #34500 showing the NBI power and the magnetic perturbation, χ_{eff} at ρ = 0.25 and ρ = 0.9 together with the ion neo-classical heat conductivity χ_{neo}(20) at the edge as calculated by TRANSP, D_α signal and total DD reaction rate R_{DD}, the central electron temperature $T_e(0)$, the plasma stored energy W_{DIA} and the line averaged electron density $\bar{n}_e$.*

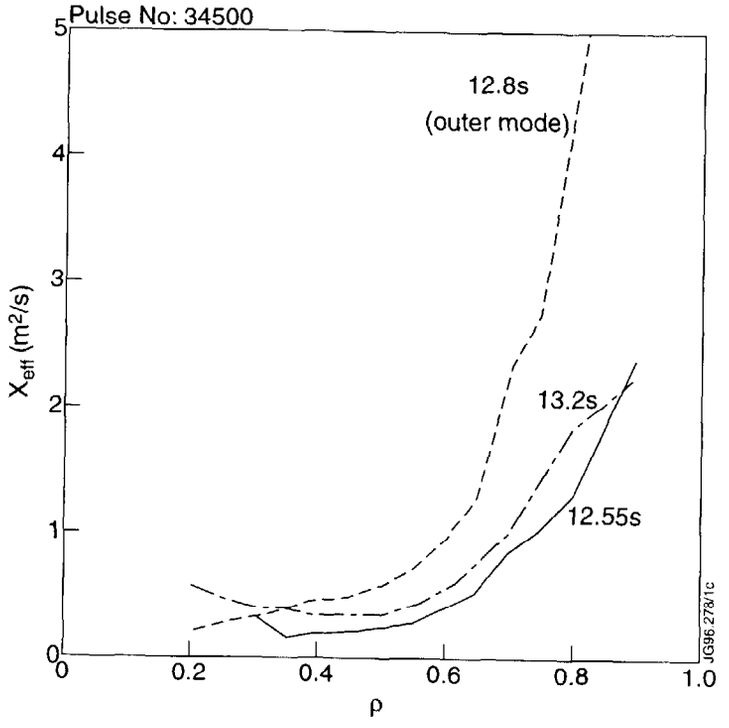

Fig. 2: χ_{eff} profiles before (t = 12.55s), during (t = 12.8s) and after (t = 13.2s) the OM for #34500.

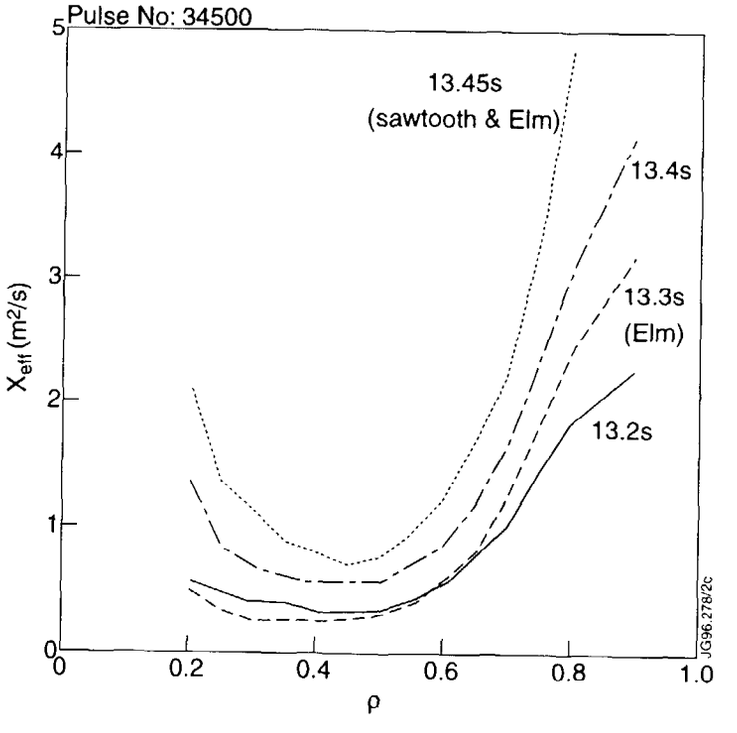

Fig. 3: χ_{eff} profiles for #34500 at different times.

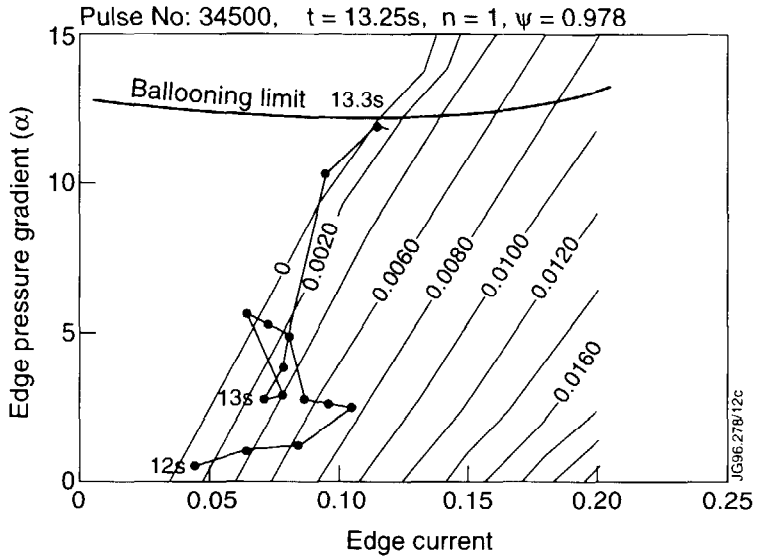

Fig. 4: Stability plot for the n = 1 kink and ballooning for #34500 at $\Psi = 0.978$.

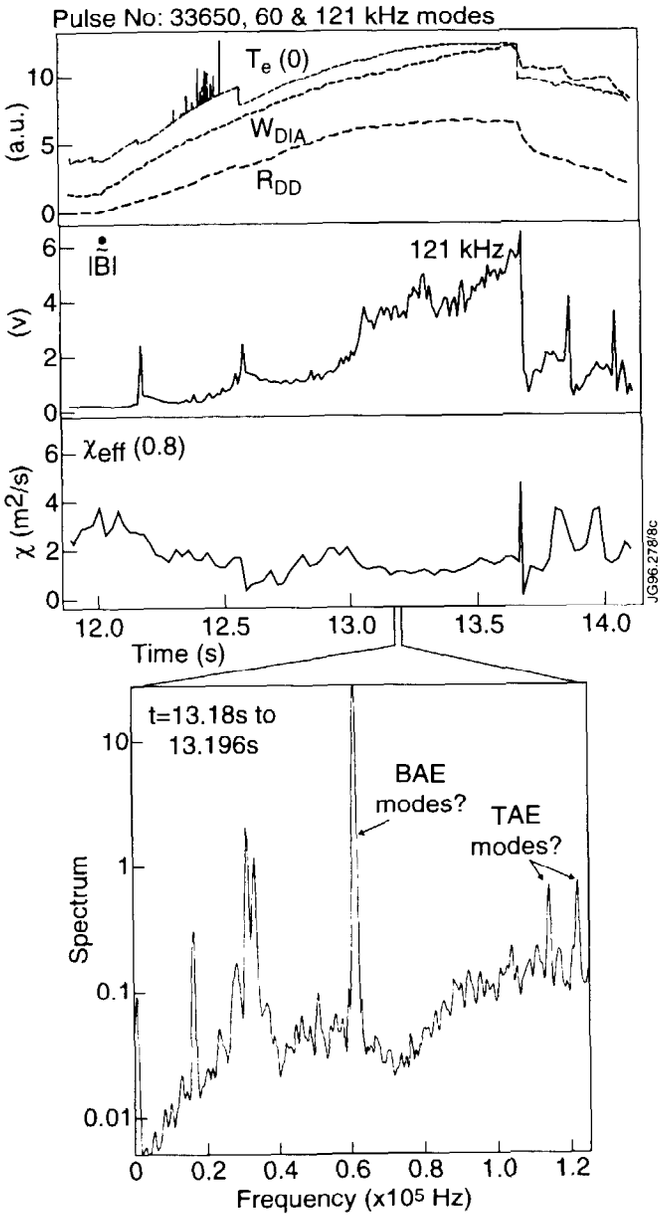

Fig. 5: Time evolution of pulse #33650 showing $T_e(0)$, W_{DIA} and R_{DD}, magnetic signals from comb filters at 121 kHz, χ_{eff} at ρ = 0.8 as calculated by TRANSP and spectrum versus frequency for t = 13.8 to 13.196s.

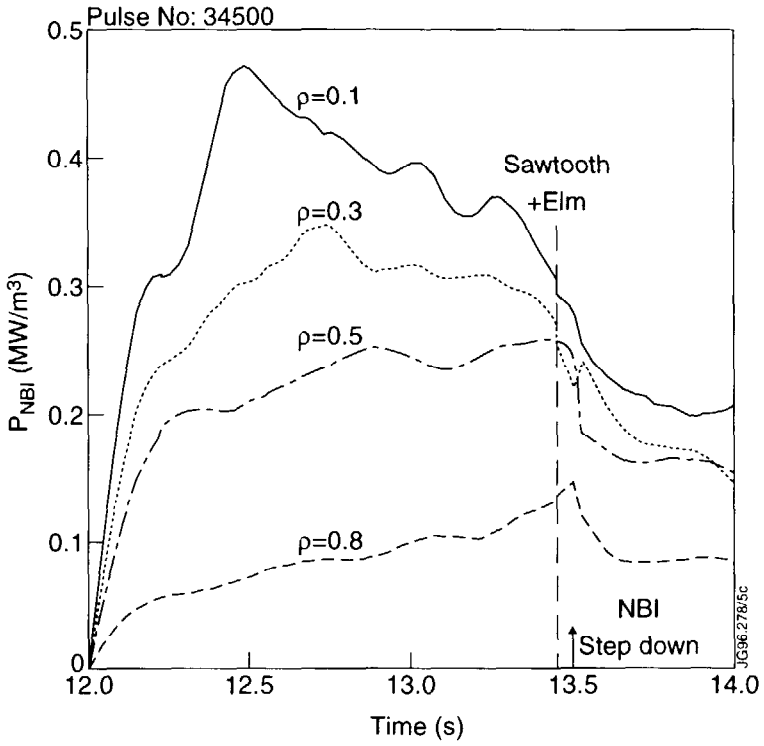

Fig. 6: Time evoultion of the absorbed NBI power density at different positions ρ for #34500.

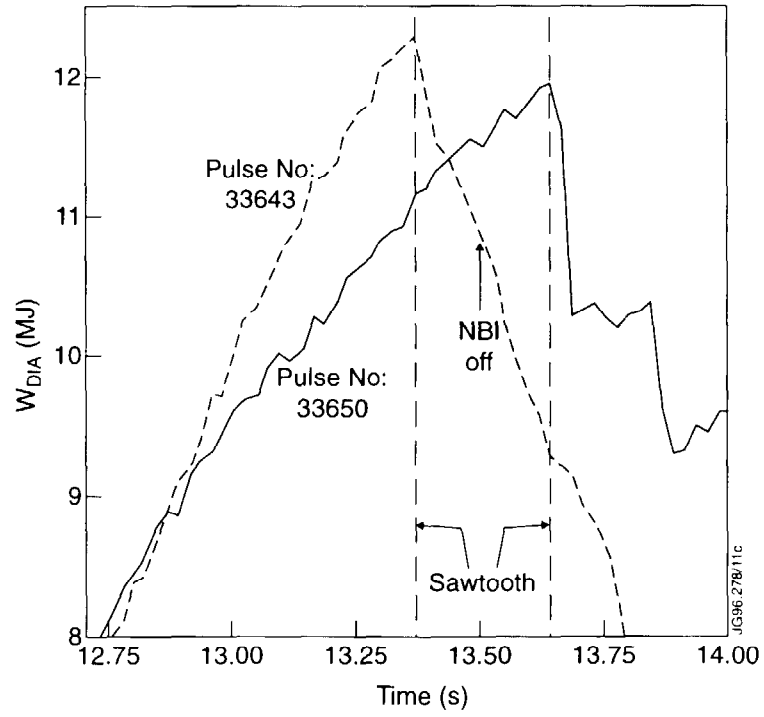

Fig. 7: Time evolution of W_{DIA} for pulses #33650 and #33643.